

# 000 001 002 003 004 005 FUSERL: DENSE PREFERENCE OPTIMIZATION FOR 006 HETEROGENEOUS MODEL FUSION 007 008 009

010 **Anonymous authors**  
011 Paper under double-blind review  
012  
013  
014  
015  
016  
017  
018  
019  
020  
021  
022  
023  
024  
025  
026

## ABSTRACT

027  
028  
029  
030  
031  
032  
033  
034  
035  
036  
037  
038  
039  
040  
041  
042  
043  
044  
045  
046  
047  
048  
049  
050  
051  
052  
053  
Heterogeneous model fusion enhances the performance of LLMs by integrating the knowledge and capabilities of multiple structurally diverse models. However, existing approaches often rely solely on selecting the best output for each prompt from source models, which underutilizes their full potential due to limited source knowledge and results in sparse optimization signals. To address this limitation, we propose FuseRL, a novel two-stage framework comprising FuseSFT and FusePO to maximize the utilization of source LLMs. FuseSFT establishes a robust initialization by integrating the strengths of heterogeneous source models through weighted supervised fine-tuning (SFT) on diverse outputs for each prompt. FusePO optimizes weighted preferences based on the outputs of multiple source models to enable superior alignment performance. Extensive experiments demonstrate the effectiveness of our framework across various preference alignment methods, including RLOO, DPO, and SimPO. Using Llama-3.1-8B-Instruct as the target model, our approach achieves competitive performance among 8B LLMs on the AlpacaEval-2 and Arena-Hard benchmarks. Further analysis suggests that FuseSFT regularizes the training to reduce overfitting, while FusePO introduces dense and diverse preference signals that enhance alignment quality.

## 1 INTRODUCTION

027  
028  
029  
030  
031  
032  
033  
034  
035  
036  
037  
038  
039  
040  
041  
042  
043  
044  
045  
046  
047  
048  
049  
050  
051  
052  
053  
Leveraging the collective knowledge and unique strengths of multiple large language models (LLMs) presents a highly promising avenue for enhancing generalization, robustness, and efficiency across a wide range of complex and diverse tasks. The underlying rationale is that no single LLM—particularly when constrained by scale or data—can comprehensively capture the full spectrum of task complexity and domain variability. Representative strategies to achieve this objective include ensemble methods (Aniol et al., 2019; Jiang et al., 2023b; Xu et al., 2024), Mixture of Experts (MoE) (Fedus et al., 2022; Sukhbaatar et al., 2024), model merging (Wortsman et al., 2022; Akiba et al., 2024), and heterogeneous model fusion (Wan et al., 2024a;b; Shi et al., 2024; Yang et al., 2024c). While these techniques share the common goal of integrating multiple LLMs to capitalize on their collective strengths, each comes with its own advantages and challenges.

027  
028  
029  
030  
031  
032  
033  
034  
035  
036  
037  
038  
039  
040  
041  
042  
043  
044  
045  
046  
047  
048  
049  
050  
051  
052  
053  
Ensemble methods combine the outputs of multiple models to generate more robust predictions. However, they typically require running all constituent models simultaneously, resulting in substantial memory and computational overhead. MoE partially alleviates these efficiency challenges by activating only a subset of parameters during inference. Nonetheless, the entire model generally remains loaded in memory, and training MoE systems can be resource-intensive. Model merging integrates models with identical architectures into a unified parameter set, enhancing robustness and generalization but limiting applicability to homogeneous model families. In contrast, heterogeneous model fusion employs techniques like multi-teacher knowledge distillation to transfer complementary expertise across diverse model configurations. However, these methods often require complex vocabulary alignment to fuse the output distributions of component models. Implicit model fusion (IMF) addresses this challenge by directly utilizing the outputs (responses) of source models for heterogeneous model fusion. For example, WRPO (Yang et al., 2024c) employs progressive adaptation to gradually shift optimization from target model outputs to high-quality source model responses.

Moreover, existing heterogeneous model fusion methods often face another critical challenge: they limit their potential by focusing exclusively on selecting the best output for each prompt from source

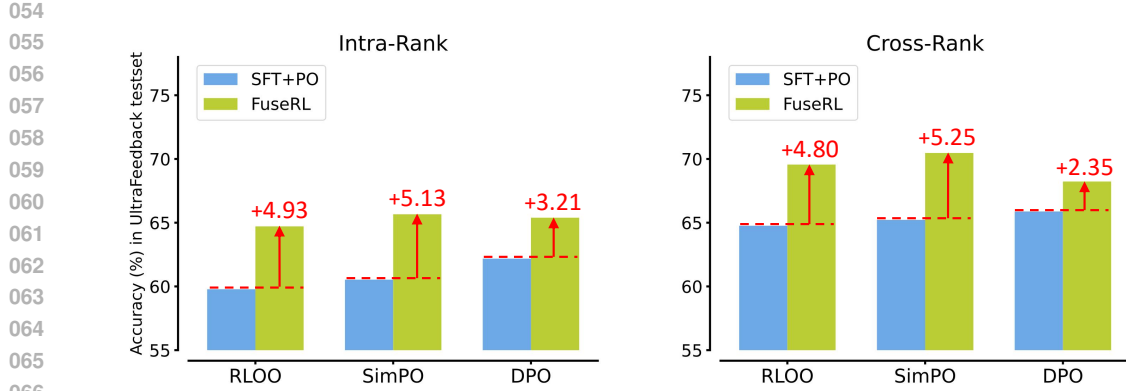


Figure 1: Effect of using a single (SFT+PO) vs. multiple (FuseRL) source LLMs for each prompt for heterogeneous model fusion on UltraFeedback (Cui et al., 2024). Accuracy (Meng et al., 2024) measures the ability to accurately distinguish between preferred and dispreferred responses by comparing the average log-probabilities assigned by different fused models. **Left:** Accuracy for multiple responses generated from a single source model. **Right:** Accuracy across responses generated by different source models. Compared to directly applying SFT followed by preference optimization (SFT+PO), FuseRL demonstrates superior performance in distinguishing responses, which reflects improved alignment with human preferences. More details are provided in Appendix D.1.

models. This narrow and static reliance on source knowledge introduces notable drawbacks, primarily stemming from bias and limited response diversity. The preferences generated by a single model reflect its unique strengths, weaknesses, and inherent response distribution, which can introduce systematic errors and restrict the variety of training data. This may result in a biased policy that overfits to the specific characteristics of that model and struggles to generalize to broader scenarios. Furthermore, the lack of diversity in source model responses limits the policy’s ability to learn from a wide range of high-quality examples, leading to sparse training signals.

This paper focuses on improving the utilization of source LLMs and providing denser, more diverse training signals for implicit model fusion. To this end, we introduce **FuseRL**, a novel reinforcement learning framework specifically designed to unlock the potential of fusing diverse source models through a two-stage process. **FuseSFT**: This stage improves the target model by fine-tuning it with high-quality responses from multiple source models. By employing a reward-based mechanism, FuseSFT prioritizes responses with high informativeness and relevance and establishes a strong foundation for subsequent fusion training. Moreover, FuseSFT effectively mitigates the *squeezing effect* (Ren & Sutherland, 2025), which can emerge during SFT and impede subsequent preference optimization. **FusePO**: Building upon the initialization from FuseSFT, FusePO aligns the target model with human preferences by dynamically leveraging weighted preference signals derived from multiple source models. This stage emphasizes high-reward preferences while maintaining adaptability across various preference optimization methods. By improving the integration of heterogeneous capabilities and maximizing the utilization of source model outputs, our framework aims to provide a more robust approach to heterogeneous model fusion. In Figure 1, we present a preliminary experiment exploring how FuseRL impacts the model’s ability to distinguish response quality. The results demonstrate that more effective utilization of diverse source models leads to richer and denser preference signals and improved alignment with human preferences.

Extensive experiments validate the effectiveness of our framework across various preference alignment methods, including RLOO, DPO, and SimPO. Our approach achieves state-of-the-art performance among 8B-sized LLMs on the AlpacaEval-2 and Arena-Hard benchmarks. Further analysis shows that fully leveraging the responses from multiple LLMs mitigates the bias introduced when relying on a single model, resulting in more diverse preference signals that better approximate the true reward distribution. Moreover, weighting preferences by their associated rewards reduces variance in the training signals by prioritizing high-quality, informative samples and down-weighting suboptimal ones. By reducing both bias and variance, the policy is able to learn from diverse data and dense signals, which in turn improves generalization and ensures stable and efficient convergence.

108 **2 PRELIMINARIES**

110 Reinforcement learning from human feedback (RLHF) (Christiano et al., 2017) is a framework for  
 111 aligning LLMs with human preferences. The training objective in RLHF is to optimize a policy  $\pi_\theta$   
 112 to maximize reward signals from human feedback while constraining excessive deviations from a  
 113 reference policy  $\pi_{\text{ref}}$ :

$$J(\pi_\theta) = \mathbb{E}_{x \sim \mathcal{D}, y \sim \pi_\theta} [r(x, y)] - \beta \text{KL}(\pi_\theta \| \pi_{\text{ref}}), \quad (1)$$

114 where  $r(x, y)$  is a reward function that captures human preferences for a prompt  $x$  and response  $y$ ,  
 115  $\text{KL}(\pi_\theta \| \pi_{\text{ref}})$  penalizes deviations of the policy  $\pi_\theta$  from the reference policy  $\pi_{\text{ref}}$ , and  $\beta$  controls the  
 116 trade-off between maximizing the overall reward and maintaining adherence to the reference policy.  
 117 This trade-off ensures stability during training and mitigates risks such as mode collapse.

118 **REINFORCE** The REINFORCE (Williams, 1992) algorithm is a classic policy gradient method  
 119 that can be adapted to implement the RLHF objective. REINFORCE updates the policy by maxi-  
 120 mizing the expected reward through gradient ascent. The policy gradient is given by:

$$\nabla_\theta J(\pi_\theta) = \mathbb{E}_{x \sim \mathcal{D}, y \sim \pi_\theta} [\nabla_\theta \log \pi_\theta(y|x) \cdot \hat{r}(x, y)], \quad (2)$$

121 where  $\hat{r}(x, y) = r(x, y) - \beta \nabla_\theta \text{KL}(\pi_\theta(\cdot|x) \| \pi_{\text{ref}}(\cdot|x))$  is the adjusted reward with KL penalty.

122 To further stabilize training, a baseline  $b$  can be introduced into the objective function of REIN-  
 123 FORCE to reduce the variance of reward estimates while maintaining their unbiased nature. REIN-  
 124 FORCE Leave-One-Out (RLOO) (Kool et al., 2019) estimates the baseline  $b$  using multiple online  
 125 samples:  $b(x, y_i) = \frac{1}{k-1} \sum_{j \neq i} \hat{r}(x, y_j)$ , where  $y_i$  represents the  $i$ th response independently sam-  
 126 pled from the policy  $\pi_\theta$  conditioned on the prompt  $x$ . With the baseline term, the adjusted reward in  
 127 Eq. (2) becomes:

$$\hat{r}(x, y) = r(x, y) - \beta \nabla_\theta \text{KL}(\pi_\theta(\cdot|x) \| \pi_{\text{ref}}(\cdot|x)) - b(x, y).$$

128 **Direct Preference Optimization (DPO)** DPO is an offline preference optimization method that  
 129 directly aligns LLMs with human preferences, offering an alternative to traditional RLHF. Unlike  
 130 RLHF, which relies on reinforcement learning to optimize a reward model and iteratively improve  
 131 the policy, DPO builds on the Bradley-Terry (BT) objective (Bradley & Terry, 1952). This objec-  
 132 tive models the probability of the preferred response  $y_w$  being ranked higher than the dispreferred  
 133 response  $y_l$ :

$$p(y_w \succ y_l|x) = \sigma(r(x, y_w) - r(x, y_l)), \quad (3)$$

134 where  $r(x, y)$  is the reward function, and  $\sigma$  is the sigmoid function. DPO reparameterizes  $r(x, y)$  in  
 135 Eq. (1) as:

$$r(x, y) = \beta \log \frac{\pi_\theta(y|x)}{\pi_{\text{ref}}(y|x)} + \beta \log Z(x), \quad (4)$$

136 where  $Z(x) = \sum_y \pi_{\text{ref}}(y|x) \exp(\frac{1}{\beta} r(x, y))$  is the partition term. From this formulation, DPO de-  
 137 fines its objective as:

$$\mathcal{L}_{\text{DPO}}(\pi_\theta; \pi_{\text{ref}}) = -\mathbb{E}_{(x, y_w, y_l) \sim \mathcal{D}} [\log p(y_w \succ y_l|x)]. \quad (5)$$

138 SimPO (Meng et al., 2024) extends DPO by introducing a reference-free reward formulation:

$$r_{\text{SimPO}}(x, y) = \frac{\beta}{|y|} \log \pi_\theta(y|x). \quad (6)$$

139 To enhance the differentiation between preferred and non-preferred responses, SimPO further intro-  
 140 duces a reward margin  $\gamma$  and modifies the BT probability as:

$$p(y_w \succ y_l|x) = \sigma(r_{\text{SimPO}}(x, y_w) - r_{\text{SimPO}}(x, y_l) - \gamma). \quad (7)$$

141 **3 METHODOLOGY**

142 To enhance the utilization of outputs from multiple source models for implicit model fusion, we  
 143 propose a novel two-stage framework, FuseRL, which consists of two key components: FuseSFT  
 144 and FusePO. FuseSFT fine-tunes the target model using high-quality responses from multiple source  
 145 models, prioritizing those with greater informativeness and relevance. FusePO further aligns the  
 146 target model with human preferences by leveraging weighted preference signals, emphasizing high-  
 147 reward responses while ensuring robustness and applicability across various preference optimization  
 148 methods. An overview of this framework is illustrated in Figure 2.

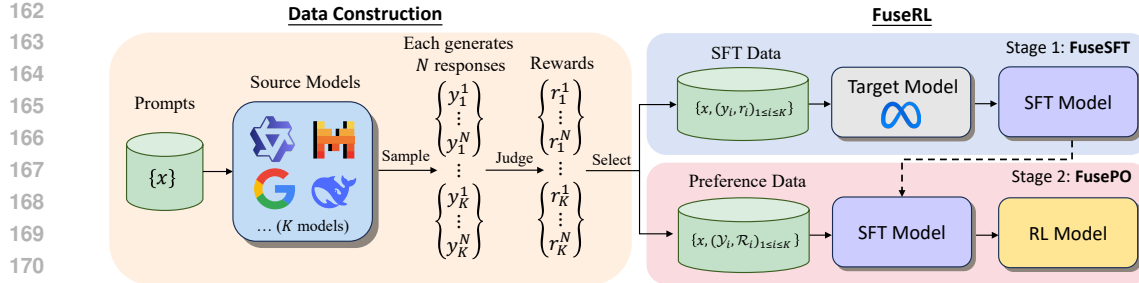


Figure 2: Overview of the proposed FuseRL framework. It comprises two stages: FuseSFT, which fine-tunes the target model using high-quality responses from diverse source models via a reward-based mechanism to prioritize informative and relevant outputs; and FusePO, which dynamically adjusts weighted preference pair contributions to align the target model with human preferences.

### 3.1 NOTATIONS

Our approach begins by constructing data samples capturing strengths of multiple source models. This ensures the target model is trained on diverse and informative responses.

Given  $K$  source models  $\mathcal{M} = \{M_1, M_2, \dots, M_K\}$ , each  $M_i$  generates a response set  $\mathcal{Y}_i$  for a given input  $x \in \mathcal{X}$ :  $\mathcal{Y}_i = \{y_i^1, y_i^2, \dots, y_i^N\}$ , for  $i = 1, 2, \dots, K$ . An external reward model is then used to assign a reward score  $r(x, y)$  to each response  $y \in \mathcal{Y}_i$ , resulting in the reward set  $\mathcal{R}_i = \{r(x, y_i^1), r(x, y_i^2), \dots, r(x, y_i^N)\}$ .

To regulate the contributions of the source models, we assign a weight to each model for a given input  $x$ . Let  $y_i = \arg \max_{y \in \mathcal{Y}_i} r(x, y)$  represent the response from source model  $M_i$  that achieves the highest reward given  $x$ . The weight for model  $M_i$  is defined as:

$$w_{x,i} = \frac{\exp(\frac{r(x,y_i)}{\alpha})}{\sum_{i=1}^K \exp(\frac{r(x,y_i)}{\alpha})}, \quad (8)$$

where  $\alpha$  is the temperature coefficient. Refer to Algorithm 1 for further details.

### 3.2 FUSESFT

Given a prompt  $x$  and response  $y$ , the supervised fine-tuning (SFT) objective for the target model  $\pi_{\theta_T}$  is defined as:

$$\mathcal{L}_{\text{SFT}}(y, x; \pi_{\theta_T}) = -\log \pi_{\theta_T}(y|x). \quad (9)$$

FuseSFT extends the standard SFT objective by utilizing responses  $\{y_i\}_{i=1}^K$  generated from all  $K$  source models to prioritize those with higher informativeness and relevance, which establishes a robust foundation for subsequent optimization. Using a similar weighting scheme as defined in Eq. (8), FuseSFT applies a weighted combination of the highest-reward responses during fine-tuning:<sup>1</sup>

$$\mathcal{L}_{\text{FuseSFT}} = \sum_{x \in \mathcal{X}} \sum_{i=1}^K w_{x,i} \cdot \mathcal{L}_{\text{SFT}}(y, x; \pi_{\theta_T}). \quad (10)$$

While FuseSFT is designed to leverage high-quality responses from multiple source models, its benefits extend beyond simple data aggregation. Recent work on learning dynamics in LLM finetuning

<sup>1</sup>The rationale for FuseSFT's modified weighting scheme is discussed in Section 4.1 and Appendix J.

(Ren & Sutherland, 2025) reveals that the early-stage supervision signal plays a critical role in shaping the model’s future behavior—especially in downstream preference optimization. Overly confident or homogeneous supervision can lead to a compression of gradient signals (the *squeezing effect*), which may adversely affect the model’s alignment performance. By incorporating diverse responses and weighting them softly rather than selecting only the highest-scoring one, FuseSFT mitigates this effect and better preserves the gradient diversity necessary for effective preference learning.

### 3.3 FUSEPO

Building on FuseSFT, FusePO aims to dynamically leverage weighted preference signals derived from multiple source models. By prioritizing high-reward preferences, it optimizes the target model using diverse and high-quality preference pairs. Moreover, FusePO employs a general preference learning loss function,  $\mathcal{L}_{\text{pref}}$ , which can be instantiated with methods such as RLOO, DPO, or others. Unlike FuseSFT, FusePO leverages the complete response set  $\mathcal{Y}_i$  from each source model to construct training data. For instance, responses from the same source model are used to create preference pairs when necessary to minimize distributional variance and enhance the overall learning process. Specifically, the FusePO loss function is defined as:

$$\mathcal{L}_{\text{FusePO}} = \sum_{x \in \mathcal{X}} \sum_{i=1}^K w_{x,i} \cdot \mathcal{L}_{\text{pref}}(\mathcal{Y}_i, \mathcal{R}_i, x; \pi_{\theta_T}). \quad (11)$$

In this work, we investigate the implementation of  $\mathcal{L}_{\text{pref}}$  using various preference optimization methods, including RLOO, DPO, and SimPO (see experiments). Furthermore, to better illustrate FuseRL, we use DPO as an example to outline the process in Algorithm 2.

## 4 EXPERIMENTS

### 4.1 EXPERIMENTAL SETUPS

**Models for fusion.** In our experiments, we utilize four diverse open-source LLMs as source models: Mistral-Large-Instruct-2407 (Jiang et al., 2023a), Gemma2-27B-IT (Riviere et al., 2024), Qwen2.5-72B-Instruct (Yang et al., 2024b), and DeepSeek-V2-Chat-0628 (Shao et al., 2024). These models were chosen for their diverse architectures, parameter scales, and complementary strengths, aligning with our goal of heterogeneous model fusion. For the target model, we employ Llama-3.1-8B-Instruct (Dubey et al., 2024) for its balance of efficiency and performance.

**Preference optimization methods.** To assess the generalizability of our FuseRL framework, we implement RLOO (Ahmadian et al., 2024), DPO (Rafailov et al., 2023), and SimPO (Meng et al., 2024) in the main experiments. RLOO serves as a traditional reinforcement learning algorithm, whereas DPO and SimPO represent reference-based and reference-free preference optimization methods, respectively. The notable distinctions among these algorithms offer a solid foundation for evaluating the adaptability of our framework.

**Baselines.** We evaluate our method with various baseline models, including proprietary LLMs, source and target LLMs, ensemble LLMs, and prior approaches for heterogeneous model fusion. Due to space limitations, detailed descriptions of all baseline settings are provided in Appendix D.2.

**Training dataset.** We utilize UltraFeedback (Cui et al., 2024) as our training dataset. UltraFeedback is a large-scale preference dataset containing approximately 64,000 samples, primarily

---

### Algorithm 2 DPO-Implemented FuseRL

**INPUT:** Target model  $\pi_{\theta_T}$ , learning rates  $\eta_{\text{sft}}$  and  $\eta_{\text{po}}$ , constructed data from Algorithm 1.

#### STAGE 1: FuseSFT

```

for each prompt  $x$  in  $\mathcal{X}_{\text{sft}}$  do
  for each source model  $M_i \in \mathcal{M}$  do
    Retrieve  $\{x, y_i, \mathcal{Y}_i, \mathcal{R}_i, w_{x,i}\}$ .
  end for
   $\theta_T \leftarrow \theta_T - \eta_{\text{sft}} \cdot \nabla_{\theta_T} \mathcal{L}_{\text{FuseSFT}}.$ 
end for

```

#### STAGE 2: FusePO

```

for each prompt  $x$  in  $\mathcal{X}_{\text{po}}$  do
  for each source model  $M_i \in \mathcal{M}$  do
    Retrieve  $\{x, y_i, \mathcal{Y}_i, \mathcal{R}_i, w_{x,i}\}$ .
    Form preference data  $(x, y_i^w, y_i^l)$  from  $\mathcal{Y}_i$  and  $\mathcal{R}_i$ .
  end for
  Minimize Eq. (11):  $\theta_T \leftarrow \theta_T - \eta_{\text{po}} \cdot \nabla_{\theta_T} \mathcal{L}_{\text{FusePO}}.$ 
end for

```

**OUTPUT:** Final fused model  $\theta_T^* \leftarrow \theta_T$ .

---

In this work, we investigate the implementation of  $\mathcal{L}_{\text{pref}}$  using various preference optimization methods, including RLOO, DPO, and SimPO (see experiments). Furthermore, to better illustrate FuseRL, we use DPO as an example to outline the process in Algorithm 2.

270  
 271 Table 1: Results of FuseRL and baselines on AlpacaEval-2 and Arena-Hard. All methods are evaluated using GPT-4-1106-Preview as the judge model. **Bolded** numbers indicate the best performance  
 272 and underlined numbers suggest the second-best performance. Scores in parentheses indicate the  
 273 points of [increase](#) or [decrease](#) relative to the counterpart in the previous row.

275 276 277 278 279 280 281 282 283 284 285 286 287 288 289 290 291 292 293 294 295 296	275 276 277 278 279 280 281 282 283 284 285 286 287 288 289 290 291 292 293 294 295 296	275 276 277 278 279 280 281 282 283 284 285 286 287 288 289 290 291 292 293 294 295 296	275 276 277 278 279 280 281 282 283 284 285 286 287 288 289 290 291 292 293 294 295 296			275 276 277 278 279 280 281 282 283 284 285 286 287 288 289 290 291 292 293 294 295 296		
			275 276 277 278 279 280 281 282 283 284 285 286 287 288 289 290 291 292 293 294 295 296	275 276 277 278 279 280 281 282 283 284 285 286 287 288 289 290 291 292 293 294 295 296	275 276 277 278 279 280 281 282 283 284 285 286 287 288 289 290 291 292 293 294 295 296	275 276 277 278 279 280 281 282 283 284 285 286 287 288 289 290 291 292 293 294 295 296	275 276 277 278 279 280 281 282 283 284 285 286 287 288 289 290 291 292 293 294 295 296	
<i>Proprietary LLMs</i>								
GPT-4o	-	57.5	51.3	1873	69.9	79.2	2988	
GPT-4-Turbo	-	50.0	50.0	2049	50.0	50.0	2748	
<i>Source&amp;Target LLMs</i>								
Llama-3.1-8B-Instruct	8B	28.3	28.7	1962	23.8	28.1	2695	
Mistral-Large-Instruct	123B	54.3	46.8	1771	63.1	70.4	1762	
Gemma2-27B-IT	27B	55.5	41.0	1558	47.4	57.5	2545	
Qwen2.5-72B-Instruct	72B	50.9	55.2	2249	63.4	78.0	3446	
DeepSeek-V2-Chat	236B	45.9	40.7	1843	58.9	68.6	2732	
<i>Ensemble LLMs</i>								
GPT4-Top1	458B	72.1	72.0	2171	92.2	94.9	3157	
LLM-Blender-Top1	458B	55.6	49.7	1857	55.9	66.2	2675	
MoA	458B	58.7	76.8	2982	72.7	87.1	4243	
<i>Heterogeneous Model Fusion</i>								
FuseLLM	8B	36.0	33.8	1930	24.6	32.1	2585	
FuseChat	8B	38.1	35.2	1866	24.8	32.7	2653	
WRPO	8B	67.7	<b>74.1</b>	2493	40.5	<u>58.1</u>	3801	
SFT	8B	41.5	38.6	1901	28.8	40.2	2831	
FuseSFT	8B	38.8 <u>(-2.7)</u>	33.7 <u>(-4.9)</u>	1805	26.4 <u>(-2.4)</u>	35.8 <u>(-4.4)</u>	2672	
SFT + RLOO	8B	59.0	63.3	2315	36.5	53.4	3324	
FuseRL <sub>RLOO</sub> (Ours)	8B	<u>67.7</u> <b>(+8.7)</b>	<u>70.6</u> <b>(+7.3)</b>	2324	40.8 <b>(+4.3)</b>	<b>58.6</b> <b>(+5.2)</b>	3523	
SFT + SimPO	8B	64.7	67.6	2269	39.8	55.6	3343	
FuseRL <sub>SimPO</sub> (Ours)	8B	<b>70.6</b> <b>(+5.9)</b>	<u>71.3</u> <b>(+3.7)</b>	2172	41.2 <b>(+1.4)</b>	56.4 <b>(+0.8)</b>	2866	
SFT + DPO	8B	67.1	69.8	2249	42.2	57.6	3360	
FuseRL <sub>DPO</sub> (Ours)	8B	<u>70.1</u> <b>(+3.0)</b>	<u>70.9</u> <b>(+1.1)</b>	2152	<b>43.7</b> <b>(+1.5)</b>	57.5 <u>(-0.1)</u>	3060	

297 focused on areas such as instruction-following, truthfulness, honesty, and helpfulness. To implement  
 298 FuseRL, we sample responses from various source models for each prompt in the dataset.  
 299 Specifically, each source model generates five responses per prompt using top- $p$  sampling (see Appendix D.3 for sampling details). These responses are then evaluated by an external reward model,  
 300 ArmoRM-Llama3-8B-v0.1 (Wang et al., 2024a).

302 We partition the dataset into two splits with a 4:6 ratio for our two-stage training process. In the  
 303 FuseSFT stage, we aggregate responses generated by the source models and select the top four  
 304 responses based on reward scores. This strategy balances diversity with the quality of training  
 305 samples. As shown in our comparative analysis in Appendix J, this selection method outperforms  
 306 selecting the best responses solely from individual source models. In the FusePO stage, due to  
 307 computational constraints, we select two responses per source model: one with the highest reward  
 308 score and one with the lowest RM score among the five sampled responses, forming  $\mathcal{Y}_i$ . Detailed  
 309 training hyperparameters and implementation specifics are provided in Appendix D.3.

310 **Evaluation.** We assess the performance of our model on two widely recognized evaluation benchmarks  
 311 in the research community: AlpacaEval-2 (Li et al., 2023; Dubois et al., 2024) and Arena-Hard  
 312 (Li et al., 2024). AlpacaEval-2 comprises 805 questions sourced from five diverse datasets. We  
 313 evaluate performance using two metrics: length-controlled (LC) win rate and raw win rate (WR),  
 314 benchmarking against GPT-4-Preview-1106. The judge model for this evaluation is also GPT-4-  
 315 Preview-1106. Arena-Hard consists of 500 challenging user queries derived from Chatbot Arena  
 316 (Chiang et al., 2024), with performance metrics including style-controlled (SC) win rate and raw win  
 317 rate (WR), compared against GPT-4-0314. The judge model employed for Arena-Hard evaluation is  
 318 GPT-4-Preview-1106. These benchmarks were selected for their capacity to comprehensively evaluate  
 319 the model’s conversational capabilities. Furthermore, we present the performance of FuseRL  
 320 across a broader range of downstream tasks, including question answering, reasoning, mathematics,  
 321 and coding. Due to space limitations, detailed results are provided in Appendix F.

## 4.2 OVERALL RESULTS

322 Table 1 presents the results of our method compared to a range of strong baseline methods on both  
 323 AlpacaEval-2 and Arena-Hard. Based on the experimental results, we identify several key insights.

324 Firstly, through our two-stage training process, FuseRL achieves substantial performance gains compared to the initial Llama-3.1-8B-Instruct (target model) on both AlpacaEval-2 and Arena-Hard benchmarks. Specifically, FuseRL<sub>DPO</sub> demonstrates an impressive 41.8-point improvement in LC win rate on AlpacaEval-2 and a 19.9-point improvement in SC win rate on Arena-Hard. Moreover, FuseRL outperforms all source LLMs and proprietary LLMs on AlpacaEval-2, including Qwen-2.5-72B-Instruct, Mistral-Large-Instruct, GPT-4-Turbo, and GPT-4o, and others.

330 Secondly, in comparison to ensemble LLM methods, FuseRL achieves higher LC win rates than both LLM-Blender-Top1 and MoA on the AlpacaEval-2 benchmark. Notably, considering that GPT4-Top1 represents a strong and sur-  
 331 posable upper bound for fusion performance (Wan et al., 2024b; Yang et al., 2024c), it is  
 332 remarkable that FuseRL closely approximates this upper bound on AlpacaEval-2, despite being  
 333 much smaller in size. However, the performance gap with GPT4-Top1 on Arena-Hard is  
 334 significantly larger. We argue that this performance discrepancy stems from inherent differ-  
 335 ences in the distribution and complexity of  
 336 prompts between UltraFeedback and Arena-  
 337 Hard, as visually illustrated in Figure 3.<sup>2</sup>

338 Thirdly, our proposed FuseRL consistently out-  
 339 performs previous heterogeneous model fusion  
 340 techniques, including FuseLLM, FuseChat, and  
 341 WRPO. Specifically, compared to the most rel-  
 342 evant baseline, WRPO, our FuseRL<sub>DPO</sub> achieves  
 343 improvements of 2.4 points on AlpacaEval-2 and  
 344 3.2 points on Arena-Hard. Furthermore, when compared to using only the best individual source  
 345 model for each prompt (i.e., SFT+RLOO, SFT+DPO, or SFT+SimPO), FuseRL delivers substantial  
 346 gains across all configurations—RLOO, DPO, and SimPO. Notably, the performance of RLOO is  
 347 comparatively lower than that of DPO and SimPO, likely due to the limited number (two) of re-  
 348 sponds used for each prompt, which constrains its overall performance. These results collectively  
 349 underscore the effectiveness of FuseRL in leveraging the dense and diverse preference signals from  
 350 heterogeneous source models to drive more robust and superior alignment performance.

### 351 4.3 FUSESFT AND FUSEPO: ABLATION STUDIES

352 Table 1 reveals another intriguing phenomenon: while the target model trained solely with SFT ini-  
 353 tially outperforms the FuseSFT model, the FuseSFT model achieves superior performance after the  
 354 second stage. Furthermore, as illustrated in  
 355 Figure 4, the target model consistently shows  
 356 improved performance after applying FuseSFT  
 357 across all (off-policy) preference optimization  
 358 methods, including DPO, SimPO, and RLOO.  
 359 This observation indicates that the alignment  
 360 performance achieved during the first stage  
 361 does not necessarily determine the eventual  
 362 performance gains realized through subsequent  
 363 preference learning. Although FuseSFT may  
 364 not yield better alignment results in the first  
 365 stage, it enhances the effectiveness of prefer-  
 366 ence learning from source models in the sec-  
 367 ond stage. We speculate that this is due to two  
 368 primary factors. First, learning from multiple  
 369 responses, rather than focusing solely on the  
 370 highest-scoring response, introduces additional  
 371 372 373 374 375 376 377

<sup>2</sup>We use all-mpnet-base-v2 from <https://huggingface.co/sentence-transformers/all-mpnet-base-v2> to generate prompt embeddings.

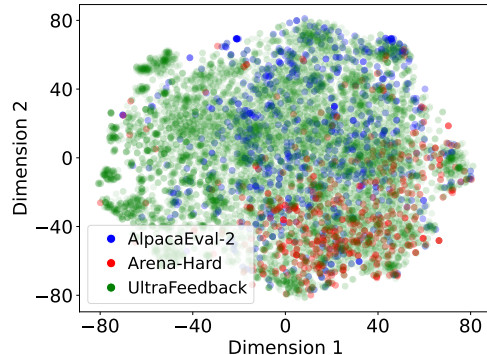


Figure 3: t-SNE visualization of prompts from UltraFeedback, AlpacaEval-2, and Arena-Hard. The prompt embeddings are projected via t-SNE. While AlpacaEval-2 prompts are distributed relatively evenly across the UltraFeedback distribution, the Arena-Hard prompts show a more pronounced distributional deviation.

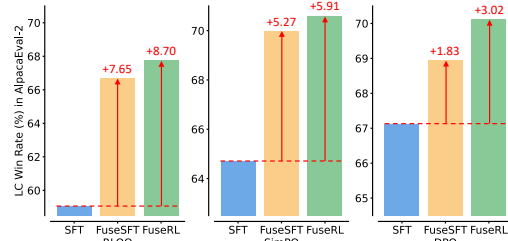


Figure 4: Ablation studies for FuseRL across various preference learning methods, including RLOO, SimPO, and DPO. SFT refers to applying standard supervised fine-tuning on the target model, while FuseSFT extends this by incorporating multiple responses from source models. FuseRL combines FuseSFT and FusePO.

378  
 379  
 380  
 381  
 382  
 383  
 384  
 385  
 386  
 Table 2: AlpacaEval-2 results of FuseRL with  
 387 varying numbers of source models (1, 2, and  
 388 4), where the number of models is the only  
 389 varying factor and all are used consistently in  
 390 both the FuseSFT and FusePO stages. The  
 391 results show that increasing the number of source  
 392 models during fusion leads to consistent im-  
 393 provements in both the LC win rate and WR.  
 394  
 395  
 396  
 397  
 398  
 399  
 400  
 401  
 402  
 403  
 404  
 405  
 406  
 407  
 408  
 409  
 410  
 411  
 412  
 413  
 414  
 415  
 416  
 417  
 418  
 419  
 420  
 421  
 422  
 423  
 424  
 425  
 426  
 427  
 428  
 429  
 430  
 431

Method	# Source Models	AlpacaEval-2	
		LC (%)	WR (%)
	4	<b>70.1</b>	<b>70.9</b>
FuseRL <sub>DPO</sub>	2	69.1	66.8
	1	65.5	62.4

challenges. FuseSFT helps regularize the training process, mitigating overfitting to preferences derived from individual source models. Second, FuseSFT enables the target model to generate more diverse responses, which benefits preference optimization in the second stage. In summary, while FuseSFT may initially fall short in delivering superior alignment results, it establishes a more robust foundation that improves preference learning in the second stage. This aligns with our earlier discussion (Section 3.2) and the findings in (Ren & Sutherland, 2025), which show that early supervision signals play a pivotal role in determining the quality of downstream preference optimization.

Furthermore, we observe that following FuseSFT, our proposed FusePO delivers consistently better results compared to existing alignment methods such as DPO. This suggests that FusePO, by effectively balancing the learning signal from diverse multi-source preference pairs, is better equipped to guide the model toward desirable behavior, leading to more robust alignment results.

#### 4.4 SCALING WITH THE NUMBER OF SOURCE MODELS

To assess the scalability of FuseRL with respect to the number of source models, we conducted a series of experiments under different configurations. In the single-source setting, we used Gemma2-27B-IT as the only source model. For the two-source configuration, we combined Gemma2-27B-IT with Mistral-Large-Instruct-2407. The four-source setup corresponds to the original FuseRL configuration, incorporating four diverse source models. The results, as summarized in Table 2, reveal a clear and consistent trend: FuseRL achieves progressively stronger alignment performance on AlpacaEval-2 as the number of source models increases from one to four. This underscores the framework’s capability to effectively integrate heterogeneous alignment signals and leverage the diversity among source models to improve overall alignment quality.

#### 4.5 EFFECT OF FUSERL ON REDUCING BIAS AND VARIANCE

To assess whether FuseRL effectively reduces bias and variance during model fusion, we conducted an experiment using DPO to compare FuseRL with the baseline fusion method (SFT+DPO), which utilizes only one source model per prompt. We analyzed the preference scores (1–2 scale) assigned by GPT-4-Preview-1106 to responses generated by the two fusion methods from AlpacaEval-2. These scores were compared against the preference scores of ideal responses to calculate bias and variance. The goal is to evaluate how the two fusion methods deviate from ideal responses. Since GPT4-Top1 is generated by selecting the top response from source model outputs for each prompt based on GPT-4-Preview-1106, it was used as the reference model to simulate ideal responses.

As shown in Figure 5, FuseRL<sub>DPO</sub> achieves lower absolute bias and variance compared to SFT+DPO. Specifically, the absolute bias and variance for FuseRL<sub>DPO</sub> are 0.010 and 0.130, while SFT+DPO shows higher values of 0.021 and 0.135. The absolute error distribution, depicted as box plots, further highlights the advantages of FuseRL<sub>DPO</sub>. The upper whisker of the box plot for FuseRL<sub>DPO</sub> is lower than SFT+DPO, indicating a tighter and more consistent error distribution. These findings demonstrate that FuseRL reduces bias and variance during the model fusion process. A theoretical analysis of the behavior is provided in Appendix E. We also conducted comparisons using SimPO and RLOO; the corresponding results are included in Appendix K.

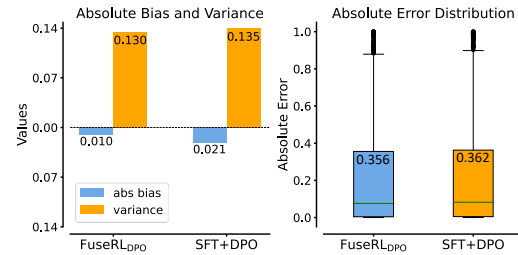


Figure 5: Results of FuseRL<sub>DPO</sub> compared to SFT+DPO on AlpacaEval-2, with preference scores provided by GPT-4-Preview-1106 using GPT4-Top1 as reference. **Left:** Absolute bias and variance. **Right:** Absolute error distribution.

432  
 433 Table 3: Comparison of FuseRL and on-policy  
 434 preference optimization methods (RLOO,  
 435 SimPO, DPO) on AlpacaEval-2. “SFT” indi-  
 436 cates that the target model first perform SFT,  
 437 followed by on-policy preference optimization.

Method	AlpacaEval-2	
	LC (%)	WR (%)
RLOO <sub>on</sub>	44.6	44.7
SFT+RLOO <sub>on</sub>	61.6	63.0
FuseRL <sub>RLOO</sub>	<b>67.7 (+6.1)</b>	<b>70.6 (+7.6)</b>
SimPO <sub>on</sub>	55.3	47.2
SFT+SimPO <sub>on</sub>	63.0	60.5
FuseRL <sub>SimPO</sub>	<b>70.6 (+7.6)</b>	<b>71.3 (+10.8)</b>
DPO <sub>on</sub>	51.7	49.6
SFT+DPO <sub>on</sub>	66.3	69.8
FuseRL <sub>DPO</sub>	<b>70.1 (+3.8)</b>	<b>70.9 (+1.1)</b>

438  
 439 Table 4: Comparison of FuseRL and the base-  
 440 line fusion method (SFT+DPO) on AlpacaEval-  
 441 2 across different model sizes (1B, 3B, 8B). The  
 442 results highlight FuseRL’s consistent gains in  
 443 both LC and WR across model scales.

Size	Method	AlpacaEval-2	
		LC (%)	WR (%)
1B	Original	9.7	10.3
	SFT + DPO	25.6	29.7
	FuseRL <sub>DPO</sub>	<b>26.8 (+1.2)</b>	<b>31.0 (+1.3)</b>
3B	Original	21.4	22.6
	SFT + DPO	47.6	50.4
	FuseRL <sub>DPO</sub>	<b>50.7 (+3.1)</b>	<b>57.9 (+7.5)</b>
8B	Original	28.3	28.7
	SFT + DPO	67.1	69.8
	FuseRL <sub>DPO</sub>	<b>70.1 (+3.0)</b>	<b>70.9 (+1.1)</b>

#### 448 449 4.6 COMPARISON TO ON-POLICY PREFERENCE OPTIMIZATION

450 Given that FuseRL leverages preference optimization for model fusion and relies on responses sam-  
 451 pled from multiple source models, we conducted experiments to compare it with traditional on-  
 452 policy preference optimization methods (Rosset et al., 2024; Meng et al., 2024), which use responses  
 453 sampled exclusively from the target model. To ensure a fairer comparison, we also experimented  
 454 with the target model to first perform SFT on the best source model for each prompt, followed  
 455 by self-sampling for preference optimization, using the same training set division as employed in  
 456 our FuseRL approach. As shown in Table 3, while on-policy methods (RLOO, SimPO, and DPO)  
 457 outperform direct SFT, their performance still falls short of that achieved by our proposed FuseRL  
 458 framework. We hypothesize that this gap arises from the lower quality of on-policy responses gen-  
 459 erated by the target model, which limits the exploration of optimal response spaces, especially when  
 460 compared to those produced by significantly larger and more capable source models. This limitation  
 461 explains why performing SFT before preference optimization mitigates the issue and highlights the  
 462 importance of FuseRL in utilizing high-quality responses from diverse source models.

#### 463 464 4.7 FUSERL ACROSS MODELS OF DIFFERENT SIZES

465 To assess the generalizability of FuseRL across different model scales, we conducted additional  
 466 experiments using Llama-3.2-1B-Instruct and Llama-3.2-3B-Instruct as the target models. These  
 467 models represent smaller scales compared to the primary 8B model, allowing us to evaluate how  
 468 well our method performs when applied to models with fewer parameters. The experimental results  
 469 in Table 4 show that FuseRL consistently achieves higher LC win rates than the baseline method  
 470 across all scales, including both the 1B and 3B models. This finding demonstrates that FuseRL’s  
 471 ability to fuse heterogeneous source models is not limited to larger target models but also transfers  
 472 to smaller-scale models. This highlights its potential to enhance alignment across diverse scales.

## 473 474 5 CONCLUSIONS

475 In this paper, we introduced FuseRL to enhance heterogeneous model fusion by maximizing the  
 476 utilization of multiple source models throughout the alignment process. FuseRL consists of two  
 477 components: FuseSFT, which integrates the strengths of diverse source models through weighted  
 478 supervised fine-tuning (SFT) to establish a robust initialization, and FusePO, which optimizes  
 479 weighted preferences from multiple source outputs to achieve superior alignment. Extensive experi-  
 480 ments demonstrate the effectiveness of FuseRL across alignment methods such as RLOO, DPO, and  
 481 SimPO, and show that it achieves promising performance among 8B-sized LLMs on AlpacaEval-  
 482 2 and Arena-Hard benchmarks. Our analysis reveals that FuseSFT regularizes the SFT process to  
 483 prevent overfitting to individual source models and reduce the detrimental squeezing effect, while  
 484 FusePO introduces diverse preference signals that enhance optimization and alignment with human  
 485 preferences. These findings highlight FuseRL as a powerful and effective approach for harnessing  
 486 heterogeneous model knowledge to enhance the optimization and alignment of LLMs.

486 ETHICS STATEMENT  
487488 The primary objective of this work is to enhance model performance by efficiently integrating het-  
489 erogeneous source models. We believe this approach holds significant potential for improving the  
490 alignment of AI systems with human preferences. Throughout the research process, we have ad-  
491 hered to responsible research practices and ethical standards. The datasets used in this study are  
492 publicly available and widely recognized within the research community, and we have verified that  
493 their use complies with all associated terms and conditions. We confirm that no conflicts of interest  
494 or sponsorships have influenced the outcomes of this work.  
495496 REPRODUCIBILITY STATEMENT  
497498 To support the reproducibility of our work, we have provided comprehensive experimental details  
499 in Section 4.1 and Appendix D.3, including data processing procedures, model configurations, and  
500 hyperparameter settings. The source code implementing the FuseRL framework is included in the  
501 supplementary materials and will be made publicly available.  
502503 REFERENCES  
504505 OpenAI Josh Achiam, Steven Adler, and et al. Sandhini Agarwal. GPT-4 technical report. *ArXiv*,  
506 abs/2303.08774, 2023.507 Arash Ahmadian, Chris Cremer, Matthias Gallé, Marzieh Fadaee, Julia Kreutzer, Olivier Pietquin,  
508 Ahmet Üstün, and Sara Hooker. Back to basics: Revisiting REINFORCE-style optimization for  
509 learning from human feedback in LLMs. In *Proceedings of the 62nd Annual Meeting of the  
510 Association for Computational Linguistics (Volume 1: Long Papers)*, pp. 12248–12267, 2024.  
511512 Takuya Akiba, Makoto Shing, Yujin Tang, Qi Sun, and David Ha. Evolutionary optimization of  
513 model merging recipes. *ArXiv*, abs/2403.13187, 2024.  
514515 Anna Aniol, Marcin Pietron, and Jerzy Duda. Ensemble approach for natural language question an-  
516 swering problem. In *Seventh International Symposium on Computing and Networking Workshops*,  
517 pp. 180–183, 2019.518 Ralph Allan Bradley and Milton E. Terry. Rank analysis of incomplete block designs: I. the method  
519 of paired comparisons. *Biometrika*, 39:324, 1952.  
520521 Wei-Lin Chiang, Lianmin Zheng, Ying Sheng, Anastasios Nikolas Angelopoulos, Tianle Li,  
522 Dacheng Li, Hao Zhang, Banghua Zhu, Michael Jordan, Joseph E Gonzalez, et al. Chatbot  
523 arena: An open platform for evaluating llms by human preference. In *International Conference  
524 on Machine Learning*, 2024.525 Paul F. Christiano, Jan Leike, Tom B. Brown, Miljan Martic, Shane Legg, and Dario Amodei. Deep  
526 reinforcement learning from human preferences. In *Advances in Neural Information Processing  
527 Systems*. Curran Associates Inc., 2017.  
528529 Ganqu Cui, Lifan Yuan, Ning Ding, Guanming Yao, Wei Zhu, Yuan Ni, Guotong Xie, Zhiyuan Liu,  
530 and Maosong Sun. UltraFeedback: Boosting language models with high-quality feedback. In  
531 *International Conference on Machine Learning*, 2024.532 Ning Ding, Yulin Chen, Ganqu Cui, Xingtai Lv, Ruobing Xie, Bowen Zhou, Zhiyuan Liu, and  
533 Maosong Sun. Mastering text, code and math simultaneously via fusing highly specialized lan-  
534 guage models. *ArXiv*, abs/2403.08281, 2024.  
535536 Abhimanyu Dubey, Abhinav Jauhri, and et al Abhinav Pandey. The llama 3 herd of models. *ArXiv*,  
537 abs/2407.21783, 2024.  
538539 Yann Dubois, Percy Liang, and Tatsunori Hashimoto. Length-controlled alpacaeval: A simple debi-  
asing of automatic evaluators. In *First Conference on Language Modeling*, 2024.

- 540 Kawin Ethayarajh, Winnie Xu, Niklas Muennighoff, Dan Jurafsky, and Douwe Kiela. KTO: Model  
 541 alignment as prospect theoretic optimization. In *International Conference on Machine Learning*,  
 542 2024.
- 543 William Fedus, Barret Zoph, and Noam Shazeer. Switch transformers: Scaling to trillion parameter  
 544 models with simple and efficient sparsity. *Journal of Machine Learning Research*, 23(120):1–39,  
 545 2022.
- 546 Aryo Pradipta Gema, Joshua Ong Jun Leang, Giwon Hong, Alessio Devoto, Alberto Carlo Maria  
 547 Mancino, Rohit Saxena, Xuanli He, Yu Zhao, Xiaotang Du, Mohammad Reza Ghasemi Madani,  
 548 Claire Barale, Robert McHardy, Joshua Harris, Jean Kaddour, Emile van Krieken, and Pasquale  
 549 Minervini. Are we done with mmlu? *ArXiv*, abs/2406.04127, 2024.
- 550 Dan Hendrycks, Collin Burns, Steven Basart, Andy Zou, Mantas Mazeika, Dawn Song, and Jacob  
 551 Steinhardt. Measuring massive multitask language understanding. In *International Conference*  
 552 *on Learning Representations*, 2021.
- 553 Jiwoo Hong, Noah Lee, and James Thorne. ORPO: Monolithic preference optimization without  
 554 reference model. In *Conference on Empirical Methods in Natural Language Processing*, 2024.
- 555 Naman Jain, King Han, Alex Gu, Wen-Ding Li, Fanjia Yan, Tianjun Zhang, Sida I. Wang, Armando  
 556 Solar-Lezama, Koushik Sen, and Ion Stoica. Livecodebench: Holistic and contamination free  
 557 evaluation of large language models for code. *ArXiv*, abs/2403.07974, 2024.
- 558 Albert Qiaochu Jiang, Alexandre Sablayrolles, Arthur Mensch, Chris Bamford, Devendra Singh  
 559 Chaplot, Diego de Las Casas, Florian Bressand, Gianna Lengyel, Guillaume Lample, Lu-  
 560 cile Saulnier, L’elio Renard Lavaud, Marie-Anne Lachaux, Pierre Stock, Teven Le Scao,  
 561 Thibaut Lavril, Thomas Wang, Timothée Lacroix, and William El Sayed. Mistral 7b. *ArXiv*,  
 562 abs/2310.06825, 2023a.
- 563 Dongfu Jiang, Xiang Ren, and Bill Yuchen Lin. LLM-blender: Ensembling large language models  
 564 with pairwise ranking and generative fusion. In *Proceedings of the 61st Annual Meeting of the*  
 565 *Association for Computational Linguistics (Volume 1: Long Papers)*, pp. 14165–14178, 2023b.
- 566 Wouter Kool, Herke van Hoof, and Max Welling. Buy 4 reinforce samples, get a baseline for  
 567 free! In *Workshop, Deep Reinforcement Learning Meets Structured Prediction, The International*  
 568 *Conference on Learning Representations*, 2019.
- 569 Woosuk Kwon, Zhuohan Li, Siyuan Zhuang, Ying Sheng, Lianmin Zheng, Cody Hao Yu, Joseph E.  
 570 Gonzalez, Hao Zhang, and Ion Stoica. Efficient memory management for large language model  
 571 serving with pagedattention. In *Proceedings of the ACM SIGOPS 29th Symposium on Operating*  
 572 *Systems Principles*, 2023.
- 573 Harrison Lee, Samrat Phatale, Hassan Mansoor, Thomas Mesnard, Johan Ferret, Kellie Ren Lu,  
 574 Colton Bishop, Ethan Hall, Victor Carbune, Abhinav Rastogi, and Sushant Prakash. RLAIF vs.  
 575 RLHF: Scaling reinforcement learning from human feedback with AI feedback. In *International*  
 576 *Conference on Machine Learning*, 2024.
- 577 Tianle Li, Wei-Lin Chiang, Evan Frick, Lisa Dunlap, Tianhao Wu, Banghua Zhu, Joseph E Gonzalez,  
 578 and Ion Stoica. From crowdsourced data to high-quality benchmarks: Arena-hard and  
 579 benchbuilder pipeline. *ArXiv*, abs/2406.11939, 2024.
- 580 Xuechen Li, Tianyi Zhang, Yann Dubois, Rohan Taori, Ishaan Gulrajani, Carlos Guestrin, Percy  
 581 Liang, and Tatsunori B. Hashimoto. AlpacaEval: An automatic evaluator of instruction-following  
 582 models, 2023. URL [https://github.com/tatsu-lab/alpaca\\_eval](https://github.com/tatsu-lab/alpaca_eval).
- 583 Tianqi Liu, Yao Zhao, Rishabh Joshi, Misha Khalman, Mohammad Saleh, Peter J Liu, and Jialu  
 584 Liu. Statistical rejection sampling improves preference optimization. In *The Twelfth International*  
 585 *Conference on Learning Representations*, 2024.
- 586 Yu Meng, Mengzhou Xia, and Danqi Chen. SimPO: Simple preference optimization with a  
 587 reference-free reward. In *Advances in Neural Information Processing Systems*, 2024.

- 594 OpenAI. Gpt-4o system card, 2024. URL <https://openai.com/index/gpt-4o-system-card/>.
- 595
- 596
- 597 Long Ouyang, Jeffrey Wu, Xu Jiang, Diogo Almeida, Carroll Wainwright, Pamela Mishkin, Chong  
598 Zhang, Sandhini Agarwal, Katarina Slama, Alex Gray, John Schulman, Jacob Hilton, Fraser Kel-  
599 ton, Luke Miller, Maddie Simens, Amanda Askell, Peter Welinder, Paul Christiano, Jan Leike,  
600 and Ryan Lowe. Training language models to follow instructions with human feedback. In *Ad-*  
601 *vances in Neural Information Processing Systems*, 2022.
- 602 Rafael Rafailov, Archit Sharma, Eric Mitchell, Christopher D Manning, Stefano Ermon, and Chelsea  
603 Finn. Direct preference optimization: Your language model is secretly a reward model. In *Ad-*  
604 *vances in Neural Information Processing Systems*, 2023.
- 605
- 606 David Rein, Betty Li Hou, Asa Cooper Stickland, Jackson Petty, Richard Yuanzhe Pang, Julien  
607 Dirani, Julian Michael, and Samuel R. Bowman. Gpqa: A graduate-level google-proof q&a  
608 benchmark. *ArXiv*, abs/2311.12022, 2023.
- 609 Yi Ren and Danica J. Sutherland. Learning dynamics of LLM finetuning. In *The Thirteenth Interna-*  
610 *tional Conference on Learning Representations*, 2025. URL <https://openreview.net/forum?id=tPNH0oZF19>.
- 611
- 612 Gemma Team Morgane Riviere, Shreya Pathak, and et al Pier Giuseppe Sessa. Gemma 2: Improving  
613 open language models at a practical size. *ArXiv*, abs/2408.00118, 2024.
- 614
- 615 Corby Rosset, Ching-An Cheng, Arindam Mitra, Michael Santacroce, Ahmed Awadallah, and  
616 Tengyang Xie. Direct nash optimization: Teaching language models to self-improve with general  
617 preferences. *ArXiv*, abs/2404.03715, 2024.
- 618
- 619 John Schulman, Filip Wolski, Prafulla Dhariwal, Alec Radford, and Oleg Klimov. Proximal policy  
620 optimization algorithms. *ArXiv*, abs/1707.06347, 2017.
- 621
- 622 Zhihong Shao, Damai Dai, Daya Guo, Bo Liu (Benjamin Liu), Zihan Wang, and Huajian Xin.  
623 DeepSeek-V2: A strong, economical, and efficient mixture-of-experts language model. *ArXiv*,  
624 abs/2405.04434, 2024.
- 625
- 626 Tianyuan Shi, Fanqi Wan, Canbin Huang, Xiaojun Quan, Chenliang Li, Mingshi Yan, and Ji Zhang.  
627 Profuser: Progressive fusion of large language models. *ArXiv*, abs/2408.04998, 2024. URL  
628 <https://api.semanticscholar.org/CorpusID:271843401>.
- 629
- 630 Zayne Rea Sprague, Xi Ye, Kaj Bostrom, Swarat Chaudhuri, and Greg Durrett. MuSR: Testing the  
631 limits of chain-of-thought with multistep soft reasoning. In *The Twelfth International Conference  
on Learning Representations*, 2024.
- 632
- 633 Sainbayar Sukhbaatar, Olga Golovneva, Vasu Sharma, Hu Xu, Xi Victoria Lin, Baptiste Roziere,  
634 Jacob Kahn, Shang-Wen Li, Wen tau Yih, Jason E Weston, and Xian Li. Branch-Train-MiX:  
635 Mixing expert LLMs into a mixture-of-experts LLM. In *First Conference on Language Modeling*,  
2024.
- 636
- 637 Leandro von Werra, Younes Belkada, Lewis Tunstall, Edward Beeching, Tristan Thrush, Nathan  
638 Lambert, Shengyi Huang, Kashif Rasul, and Quentin Gallouédec. TRL: Transformer reinforce-  
639 ment learning, 2020. URL <https://github.com/huggingface/trl>.
- 640
- 641 Fanqi Wan, Xinting Huang, Deng Cai, Xiaojun Quan, Wei Bi, and Shuming Shi. Knowledge fusion  
642 of large language models. In *The Twelfth International Conference on Learning Representations*,  
2024a.
- 643
- 644 Fanqi Wan, Ziyi Yang, Longguang Zhong, Xiaojun Quan, Xinting Huang, and Wei Bi. FuseChat:  
645 Knowledge fusion of chat models. *ArXiv*, abs/2402.16107, 2024b.
- 646
- 647 Haoxiang Wang, Wei Xiong, Tengyang Xie, Han Zhao, and Tong Zhang. Interpretable preferences  
via multi-objective reward modeling and mixture-of-experts. In *Conference on Empirical Meth-*  
648 *ods in Natural Language Processing*, 2024a.

- 648 Junlin Wang, Jue Wang, Ben Athiwaratkun, Ce Zhang, and James Zou. Mixture-of-agents enhances  
 649 large language model capabilities. *ArXiv*, abs/2406.04692, 2024b.  
 650
- 651 Yubo Wang, Xueguang Ma, Ge Zhang, Yuansheng Ni, Abhranil Chandra, Shiguang Guo, Weiming  
 652 Ren, Aaran Arulraj, Xuan He, Ziyian Jiang, Tianle Li, Max W.F. Ku, Kai Wang, Alex Zhuang,  
 653 Rongqi "Richard" Fan, Xiang Yue, and Wenhui Chen. Mmlu-pro: A more robust and challenging  
 654 multi-task language understanding benchmark. *ArXiv*, abs/2406.01574, 2024c.
- 655 Johannes Welbl, Nelson F. Liu, and Matt Gardner. Crowdsourcing multiple choice science questions.  
 656 *ArXiv*, abs/1707.06209, 2017.
- 657
- 658 Ronald J Williams. Simple statistical gradient-following algorithms for connectionist reinforcement  
 659 learning. *Machine learning*, 8:229–256, 1992.
- 660 Mitchell Wortsman, Gabriel Ilharco, Samir Ya Gadre, Rebecca Roelofs, Raphael Gontijo-Lopes,  
 661 Ari S Morcos, Hongseok Namkoong, Ali Farhadi, Yair Carmon, Simon Kornblith, et al. Model  
 662 soups: averaging weights of multiple fine-tuned models improves accuracy without increasing  
 663 inference time. In *International Conference on Machine Learning*, 2022.
- 664 Yangyifan Xu, Jinliang Lu, and Jiajun Zhang. Bridging the gap between different vocabularies  
 665 for LLM ensemble. In *Proceedings of the 2024 Conference of the North American Chapter of  
 666 the Association for Computational Linguistics: Human Language Technologies (Volume 1: Long  
 667 Papers)*, pp. 7140–7152, June 2024.
- 668
- 669 An Yang, Beichen Zhang, Binyuan Hui, Bofei Gao, Bowen Yu, Chengpeng Li, Dayiheng Liu,  
 670 Jianhong Tu, Jingren Zhou, Junyang Lin, Keming Lu, Mingfeng Xue, Runji Lin, Tianyu Liu,  
 671 Xingzhang Ren, and Zhenru Zhang. Qwen2.5-math technical report: Toward mathematical ex-  
 672 pert model via self-improvement. *ArXiv*, abs/2409.12122, 2024a.
- 673 Qwen An Yang, Baosong Yang, and et al Beichen Zhang. Qwen2.5 technical report. *ArXiv*,  
 674 abs/2412.15115, 2024b.
- 675
- 676 Ziyi Yang, Fanqi Wan, Longguang Zhong, Tianyuan Shi, and Xiaojun Quan. Weighted-reward  
 677 preference optimization for implicit model fusion. *ArXiv*, abs/2412.03187, 2024c.
- 678 Rowan Zellers, Ari Holtzman, Yonatan Bisk, Ali Farhadi, and Yejin Choi. HellaSwag: Can a ma-  
 679 chine really finish your sentence? In *Proceedings of the 57th Annual Meeting of the Association  
 680 for Computational Linguistics*, pp. 4791–4800, 2019.
- 681
- 682
- 683
- 684
- 685
- 686
- 687
- 688
- 689
- 690
- 691
- 692
- 693
- 694
- 695
- 696
- 697
- 698
- 699
- 700
- 701

702 **A LIMITATIONS**

703  
 704 While FuseRL demonstrates strong empirical performance, it also has several limitations. First, the  
 705 framework relies on an external reward model to assess and weight responses from source models.  
 706 As a result, the quality of the training signal is sensitive to the alignment and calibration of the reward  
 707 model. Second, due to resource constraints, the evaluation was conducted on a limited set of source  
 708 models. The applicability of FuseRL to a broader range of models, including both open-source and  
 709 commercial LLMs with greater diversity, remains an open direction for future investigation.

710 **B STATEMENT ON THE USE OF LARGE LANGUAGE MODELS**

711  
 712 In this work, large language models were utilized solely for the purpose of polishing the manuscript.  
 713 Specifically, they were employed to improve clarity and precision of phrasing, ensure grammatical  
 714 correctness and spelling accuracy, and provide suggestions to enhance overall coherence and  
 715 readability. The core research problem, conceptual framework, methodologies, experimental de-  
 716 sign, analysis, and result interpretation are entirely developed by the authors. The use of LLMs is  
 717 strictly confined to improving the efficiency and quality of academic writing without influencing the  
 718 intellectual contributions of this work.

719 **C RELATED WORK**

720 This work is closely related to alignment techniques for LLMs, as well as collective approaches like  
 721 model ensembling and heterogeneous model fusion.

722 **LLMs alignment** Aligning large language models (LLMs) with human expectations using tech-  
 723 niques such as reinforcement learning from human feedback (RLHF) (Christiano et al., 2017) is a  
 724 critical step in developing effective and safe LLMs. InstructGPT (Ouyang et al., 2022) employs  
 725 a three-stage pipeline that includes supervised fine-tuning, reward model training, and policy op-  
 726 timization via proximal policy optimization (PPO) (Schulman et al., 2017). However, this multi-  
 727 stage process is costly, complex, and potentially unstable. To address these challenges, researchers  
 728 have explored various improvements. For instance, Ahmadian et al. (2024) showed that simpli-  
 729 fied reinforcement learning methods such as REINFORCE (Williams, 1992) can achieve alignment  
 730 effectively without relying on advanced optimization components like value-function critics and ad-  
 731 vantage estimation. Similarly, reinforcement learning from AI feedback (RLAIF) (Lee et al., 2024)  
 732 offers a cost-effective alternative to relying on expensive human-labeled data by utilizing preference  
 733 labels generated by LLMs, while achieving comparable performance to traditional RLHF methods.

734 Direct Preference Optimization (DPO) (Rafailov et al., 2023) simplifies the RLHF process by di-  
 735 rectly optimizing the policy using human preference data, eliminating the need for an explicit reward  
 736 model and offering improved training stability. However, DPO faces challenges, such as its reliance  
 737 on a reference model, susceptibility to overfitting on noisy preference data, and managing the trade-  
 738 off between exploration and exploitation. ORPO (Hong et al., 2024) addresses the dependency of  
 739 DPO on a reference model by incorporating odds ratios into the supervised fine-tuning process, al-  
 740 lowing models to directly distinguish between preferred and dispreferred outputs. KTO (Ethayarajh  
 741 et al., 2024) introduces a human-aware loss (HALO) to maximize the utility of model generations  
 742 using a binary signal indicating desirability, rather than focusing on preference likelihoods. Sim-  
 743ilarly, RSO (Liu et al., 2024) enhances preference optimization by sourcing data pairs from the  
 744 estimated optimal policy through rejection sampling. Recently, SimPO (Meng et al., 2024) further  
 745 streamlines DPO by leveraging the average log-probability of sequences as an implicit reward and  
 746 introducing a reward margin to better differentiate between positive and negative responses.

747 **Collective LLMs** Collective LLMs aim to enhance the performance of LLMs by integrating  
 748 knowledge and capabilities from multiple models. As a representative ensemble method, LLM-  
 749 Blender (Jiang et al., 2023b) performs pairwise ranking of candidate outputs, selecting and ag-  
 750 gregating the most promising responses into a superior output using a sequence-to-sequence model.  
 751 Similarly, Mixture-of-Agents (MoA) (Wang et al., 2024b) employs a multi-layer architecture, where  
 752 LLM agents in each layer iteratively refine responses based on the outputs of the previous layer,  
 753 gradually improving generation quality. UltraFuser (Ding et al., 2024) leverages three expert models  
 754 trained on language, code, and mathematics tasks, and combines their outputs through a token-level  
 755 gating mechanism to dynamically select the most relevant expertise for each task. Branch-Train-  
 MiX (BTX) (Sukhbaatar et al., 2024) employs a parallel training strategy to train multiple expert

756 models starting from a shared seed model, which are combined into a Mixture of Experts (MoE)  
 757 framework. The resulting MoE model is then fine-tuned to optimize token-level routing decisions  
 758 and maximize the utilization of each expert’s capabilities.

759 Heterogeneous model fusion aims to transfer the capabilities of multiple source models into a single  
 760 target model. These approaches can be broadly classified as explicit or implicit. Explicit model  
 761 fusion (EMF) methods, such as FuseLLM (Wan et al., 2024a) and FuseChat (Wan et al., 2024b),  
 762 utilize knowledge distillation to explicitly transfer knowledge, typically in the form of probabilis-  
 763 tic distribution matrices, from multiple source models to a single target model. FuseLLM employs  
 764 a multi-teacher distillation strategy for this transfer, whereas FuseChat adopts a fuse-and-merge  
 765 framework. In FuseChat, pairwise knowledge fusion is first conducted between each source model  
 766 and a pivot model to produce multiple target models with identical structure and size. These tar-  
 767 get models are then merged within the parameter space to complete the process. WRPO (Yang  
 768 et al., 2024c) introduces implicit model fusion (IMF), where the target model leverages high-quality  
 769 responses generated by source models as auxiliary signals during preference optimization. How-  
 770 ever, WRPO focuses solely on selecting the highest-reward output for each prompt, which limits the  
 771 utilization of the broader knowledge from all source models. This neglect of the diverse and rich  
 772 signals from source LLMs may limit the effectiveness of model fusion.

## 773 D IMPLEMENTATION DETAILS

### 774 D.1 DETAILS OF PRELIMINARY EXPERIMENTS

775 In this section, we provide a detailed description of the experimental setup used in our prelim-  
 776 inary experiments, with the results illustrated in Figure 1. The data construction process for these  
 777 preliminary experiments mirrors that of the main experiment described in Section 4.1, utilizing  
 778 the same four source models and reward model. For each prompt in the UltraFeedback test set  
 779 (Cui et al., 2024), each source model generates five responses, which are then scored by the re-  
 780 ward model, ArmoRM-Llama3-8B-v0.1 (Wang et al., 2024a). We compare our proposed method,  
 781 FuserL, against SFT+PO, which serves as a baseline implementation of our approach. Specifically,  
 782 SFT+PO incorporates only a single response during supervised fine-tuning (SFT) or a single pre-  
 783 ference pair during preference optimization (PO) for each prompt. In this context, we explore pre-  
 784 ference optimization using a range of techniques, including RLOO (Ahmadian et al., 2024), SimPO  
 785 (Meng et al., 2024), and DPO (Rafailov et al., 2023).

786 To evaluate the impact of FuserL on the model’s ability to distinguish response quality, we con-  
 787 duct two types of evaluations: Intra-Rank and Cross-Rank. The Intra-Rank evaluation examines the  
 788 model’s ability to distinguish response quality within a *single* source model, while the Cross-Rank  
 789 evaluation assesses its ability to distinguish response quality across *different* source models. In the  
 790 **Intra-Rank** evaluation, for each source model, the reward model identifies the response with the  
 791 highest reward  $y_w$  and the one with the lowest reward  $y_l$ . Following previous study (Meng et al.,  
 792 2024), the model under evaluation computes the average log probability for each response as its  
 793 predicted reward score  $r_m(y)$ . It is important to note that for DPO and RLOO, the computation of  
 794 rewards during evaluation differs from their training phase but remains consistent with their infer-  
 795 ence phase. To ensure fairness, we adopt the same approach described above for all three methods:  
 796 RLOO, SimPO, and DPO. We then check whether  $r_m(y_w) > r_m(y_l)$  and calculate the accuracy as  
 797 the ratio of correct matches to the total number of samples in the test set for each source model. The  
 798 final result is obtained by averaging the accuracy across all source models. As for the **Cross-Rank**  
 799 evaluation, we select one response from each source model for each test prompt. The reward model  
 800 then identifies the response with the highest reward  $y_w$  and the response with the lowest reward  $y_l$ .  
 801 We verify whether  $r_m(y_w) > r_m(y_l)$  following the same process as the Intra-Rank evaluation and  
 802 calculate the accuracy as the ratio of correct matches to the total number of samples in the test set.

### 803 D.2 DETAILS OF BASELINES

804 We evaluate our method against various baseline models: proprietary LLMs, source and target  
 805 LLMs, ensemble LLMs, and heterogeneous model fusion approaches.

806 **Proprietary LLMs:** We evaluate closed-source models, including GPT-4o (OpenAI, 2024), GPT-  
 807 4-Turbo (Achiam et al., 2023). We prioritize results from official sources.

810     **Source and Target LLMs:** The evaluation strategy mirrors that used for Proprietary LLMs, relying  
 811     on official results when available and locally evaluated results otherwise.  
 812

813     **Ensemble LLMs:** Ensemble LLMs leverage multiple models to enhance performance through vari-  
 814     ous collaborative approaches. In this study, we examine several methods for utilizing responses from  
 815     our source LLMs. The GPT4-Top1 (Achiam et al., 2023) provides an upper performance bound by  
 816     ranking the responses from source models based on GPT-4’s evaluations and selecting the best one.  
 817     Similarly, LLM-Blender-Top1 (Jiang et al., 2023b) employs a ranking mechanism to choose the  
 818     optimal response from multiple LLM outputs. Alternatively, the MoA (Wang et al., 2024b) uses  
 819     Qwen2.5-72B-Instruct as an aggregator to integrate responses and produce a unified output.  
 820

821     **Heterogeneous Model Fusion.** FuseLLM (Wan et al., 2024a) and FuseChat (Wan et al., 2024b)  
 822     adopt knowledge distillation techniques to transfer knowledge from multiple source models to a  
 823     target model. Due to computational constraints, we did not reproduce these results using our specific  
 824     source and target models. Instead, we rely on the results reported by Yang et al. (2024c), while noting  
 825     minor differences in the number and versions of the source models used. Furthermore, we compare  
 826     our approach with WRPO (Yang et al., 2024c), the work most closely related to ours.  
 827

### 828     D.3 DETAILS OF HYPERPARAMETERS

829     All our experiments were conducted using the TRL (von Werra et al., 2020) library. The Ultra-  
 830     Feedback (Cui et al., 2024) dataset was randomly divided into two subsets in a 4:6 ratio for the  
 831     two-stage training process. For on-policy implementation, all samples were directly used for training.  
 832     A batch size of 128 and a maximum sequence length of 2048 were applied across all stages.  
 833

834     During the SFT/FuseSFT stage, training was  
 835     performed over 3 epochs. The learning rate  
 836     was selected through a search over the range  
 837     [1e-6, 7e-6, 1e-5, 2e-5], with 7e-6 chosen  
 838     for SFT and 1e-5 for FuseSFT. For the Fus-  
 839     eSFT/FusePO stage, the temperature parame-  
 840     ter was explored within the range [1e-1, 1e-2,  
 841     5e-3, 1e-3, 1e-4], with 1e-2 chosen for Fus-  
 842     eSFT, 5e-3 for FuseRL<sub>DPO</sub> and FuseRL<sub>RLOO</sub>,  
 843     and 1e-3 for FuseRL<sub>SimPO</sub>. For the imple-  
 844     mentation of RLOO in the TRL library, a KL  
 845     penalty is essential to prevent training col-  
 846     lapse. The KL coefficient was selected from  
 847     the range [1e-4, 1e-3, 1e-2, 1e-1]. In the pref-  
 848     erence optimization stage, the search strate-  
 849     gy from SimPO (Meng et al., 2024) was fol-  
 850     lowed. The learning rate search range for all  
 851     preference learning algorithms was [3e-7, 5e-  
 852     7, 6e-7, 8e-7, 1e-6].  
 853

854     The best hyperparameter settings for some  
 855     baselines and FuseRL are summarized in Ta-  
 856     ble 5. For response collection, we utilized the  
 857     vLLM library (Kwon et al., 2023). The sam-  
 858     pling parameters for each source model were configured based on their default generation settings.  
 859     Detailed sampling parameters for the various source models are provided in Table 6. All experiments  
 860     were conducted on a computing cluster equipped with 8x80G NVIDIA A800 GPUs.  
 861

## 862     E THEORETICAL ANALYSIS

863     We conduct a theoretical analysis of FuseSFT and FusePO to illustrate how reward-based weighting  
 864     aggregation enhances the robustness and effectiveness of the FuseRL framework.  
 865

866     **Proposition 1.** *In both FuseSFT and FusePO, reward-based weighting emphasizes  
 867     responses with higher weights during parameter updates, progressively guiding the target model to  
 868     prioritize high-quality responses throughout fine-tuning and preference optimization.*

864 *Proof.* Consider the loss functions defined in Eq. (10) and Eq. (11). In both cases, the loss is  
 865 represented as a weighted sum of model-specific losses, with the weights determined by  $w_{x,i}$ . For  
 866 ease of analysis, we introduce a unified notation  $\mathcal{L}$ , which represents both  $\mathcal{L}_{\text{soft}}$  and  $\mathcal{L}_{\text{pref}}$ . Moreover,  
 867 we use  $\mathcal{L}_i$  to denote the model-specific loss component within the two loss functions. Therefore, the  
 868 gradient of the loss  $\mathcal{L}$  with respect to model parameters  $\theta_T$  is given by:  
 869

$$\nabla_{\theta_T} \mathcal{L} = \sum_{x \in \mathcal{X}} \sum_{i=1}^K w_{x,i} \cdot \nabla_{\theta_T} \mathcal{L}_i. \quad (12)$$

872 Since  $w_{x,i}$  is derived from a softmax function, source models with higher maximum rewards are  
 873 assigned exponentially larger weights. This amplifies the scaling of their corresponding gradients,  
 874  $\nabla_{\theta_T} \mathcal{L}_i$ , by larger factors. As a result, these high-weighted terms dominate the overall gradient,  
 875 steering parameter updates to prioritize minimizing the loss associated with high-reward responses.  
 876 Furthermore, we note that the parameter updates also depend on the magnitude of  $\nabla_{\theta_T} \mathcal{L}_i$ . If a  
 877 highly weighted term has a small gradient, its influence on the parameter updates may be limited.  
 878 Nevertheless, the weighted aggregation naturally amplifies the relative importance of high-reward  
 879 terms, ensuring they receive greater attention during optimization.

880 **Proposition 2.** *Under the assumptions that the biases introduced by different source models are  
 881 independent and identically distributed (i.i.d.) for each input  $x \in \mathcal{X}$ , aggregating and weighting  
 882 responses or preference pairs from multiple source models preserves the expected bias of individual  
 883 models and strictly reduces their variance.*

884 *Proof.* Let  $\epsilon_{x,i}$  represent the bias introduced by source model  $M_i$  for a given input  $x \in \mathcal{X}$ . The  
 885 aggregated influence of these biases on the gradient update is:  
 886

$$\epsilon_{\text{agg}}(x) = \sum_{i=1}^K w_{x,i} \cdot \epsilon_{x,i}. \quad (13)$$

887 Since these biases are independent and identically distributed, it follows that  $\mathbb{E}[\epsilon_{x,i}] = \mu$  and  
 888  $\text{Var}(\epsilon_{x,i}) = \sigma^2$ .  
 889

890 The expected value of the aggregated bias is the sum of the expected values of each weighted bias:  
 891

$$\begin{aligned} \mathbb{E}[\epsilon_{\text{agg}}(x)] &= \mathbb{E}\left[\sum_{i=1}^K w_{x,i} \cdot \epsilon_{x,i}\right] \\ &= \sum_{i=1}^K w_{x,i} \cdot \mathbb{E}[\epsilon_{x,i}] = \mu \sum_{i=1}^K w_{x,i} = \mu. \end{aligned} \quad (14)$$

892 The variance of the aggregated bias is given by:  
 893

$$\text{Var}(\epsilon_{\text{agg}}(x)) = \text{Var}\left(\sum_{i=1}^K w_{x,i} \cdot \epsilon_{x,i}\right) = \sum_{i=1}^K w_{x,i}^2 \cdot \text{Var}(\epsilon_{x,i}). \quad (15)$$

901 Since  $w_{x,i}$  are weights derived from softmax normalization, we have  $0 < w_{x,i} < 1$  and  $\sum_{i=1}^K w_{x,i} = 1$ . Therefore,  $w_{x,i}^2 < w_{x,i}$ , and summing over all  $i$  yields:  
 902

$$\sum_{i=1}^K w_{x,i}^2 < \sum_{i=1}^K w_{x,i} = 1. \quad (16)$$

903 Thus, by combining Equations (15) and (16), we obtain:  
 904

$$\text{Var}\left(\sum_{i=1}^K w_{x,i} \cdot \epsilon_{x,i}\right) < \text{Var}(\epsilon_{x,i}) = \sigma^2. \quad (17)$$

915 For every input  $x$ , the expected value of the aggregated bias  $\epsilon_{\text{agg}}(x)$  remains equal to the expectation  
 916 of the individual biases,  $\mu$ , ensuring that the aggregation process preserves the systematic bias.  
 917 Moreover, the variance of the aggregated bias is strictly less than  $\sigma^2$ , demonstrating that aggregating  
 918 and weighting the biases effectively reduces variance.

918  
919  
920  
921 Table 7: Evaluation results of FuseRL on various downstream tasks.  
922  
923  
924  
925  
926  
927

Dataset (→)	HellaSwag	MuSR	MMLU-Pro	GPQA Diamond	SciQ	MMLU-Redux	AMC 23	LiveCodeBench (2408-2411)	Avg.
Setup (→)	10-shot Acc Norm	0-shot Acc Norm	5-shot Acc	0-shot Acc Norm	0-shot Acc Norm	0-shot Acc	0-shot, CoT Acc	0-shot Pass @ 1	
Llama-3.1-8B-Instruct	80.2	35.7	33.6	33.8	96.0	67.2	25.0	12.3	53.1
SFT	62.3	38.8	36.7	31.8	92.4	68.6	27.5	11.3	51.2
FuseSFT	80.8	39.4	35.2	31.3	96.3	65.0	17.5	10.0	52.2
SFT + DPO	83.6	34.7	37.1	29.3	87.1	68.4	25.0	11.3	52.2
SFT + WRPO	84.1	33.7	36.5	28.8	94.6	66.3	17.5	9.4	51.6
FuseRL-DPO	82.0	34.9	34.7	33.3	95.7	66.5	27.5	12.5	53.5

928  
929  
930 F DOWNSTREAM TASK EVALUATION  
931932 To assess FuseRL’s impact on downstream tasks, we conducted experiments on eight downstream  
933 tasks spanning general knowledge, mathematics, and coding. These tasks are described as follows:  
934935 **HellaSwag** (Zellers et al., 2019): A commonsense reasoning benchmark requiring models to choose  
936 the most plausible continuation of a given context.937 **MuSR** (Sprague et al., 2024): A dataset comprising algorithmically generated complex problems,  
938 such as murder mysteries, object placement challenges, and team allocation optimizations. These  
939 tasks require advanced reasoning skills and the ability to parse long-range context effectively.940 **MMLU-Pro** (Wang et al., 2024c): An enhanced version of MMLU (Hendrycks et al., 2021), which  
941 is a multiple-choice dataset to evaluate knowledge capability. This dataset is designed to address  
942 issues such as noisy data and reduced difficulty due to advances in model capabilities and increased  
943 data contamination. MMLU-Pro increases challenge levels by expanding multiple-choice options  
944 from 4 to 10, requiring reasoning across more questions, and incorporating expert-reviewed annotations  
945 for improved quality and reduced noise.946 **GPQA Diamond** (Rein et al., 2023): A challenging knowledge benchmark crafted by PhD-level  
947 domain experts in biology, physics, and chemistry. The dataset contains questions that are straight-  
948 forward for experts but difficult for laypersons. We evaluate on the highest quality diamond set  
949 comprising 198 questions.950 **SciQ** (Welbl et al., 2017): A collection of 13.7k multiple-choice questions derived from science  
951 exams, covering a broad range of scientific topics.953 **MMLU-Redux** (Gema et al., 2024): A re-annotated subset of the MMLU (Hendrycks et al., 2021)  
954 dataset created through manual assessment from 14 human experts.955 **AMC 23** (Yang et al., 2024a): The 2023 American Mathematics Competition, featuring 25 multiple-  
956 choice questions that test advanced high school mathematics, including trigonometry, advanced al-  
957 gebra, and elements of calculus.958 **LiveCodeBench (2408-2411)** (Jain et al., 2024): A benchmark designed to evaluate coding ca-  
959 pabilities using an evolving set of contamination-free problems sourced from platforms including  
960 LeetCode, AtCoder, and CodeForces. We evaluate on the subset comprising 160 problems published  
961 between August 2024 and November 2024.962 The results presented in Table 7 offer several important insights. Both SFT and FuseSFT lead  
963 to a decline in general performance. This decrease can be attributed to the fact that our train-  
964 ing dataset primarily emphasizes preference alignment, suggesting an inherent trade-off between  
965 preference alignment and overall model performance. Although FuseSFT does not surpass SFT  
966 in alignment performance, it performs better at preserving the model’s general capabilities. This  
967 highlights FuseSFT’s strength in balancing human preference alignment while maintaining broader  
968 performance. After the preference alignment stage, a slight improvement in general performance is  
969 observed across the models. However, with the exception of FuseRL, all models perform worse than  
970 the target model. Interestingly, the average performance of FuseRL exceeds that of the target model,  
971 albeit by a small margin. This indicates that FuseRL not only improves preference alignment but  
also effectively maintains general performance.

## 972 G TRAINING COST ANALYSIS FOR MODEL FUSION 973

974 FuseRL is designed with a scalable data strategy that enables efficient use of training resources  
975 while maintaining strong performance. In particular, our framework supports data scaling along two  
976 complementary dimensions: the number of prompts and the number of responses per prompt. This  
977 dual-scaling mechanism allows the model to benefit from a richer distribution of supervision signals  
978 without proportionally increasing the cost of data preparation.

979 Notably, scaling the number of responses is relatively efficient—it only requires sampling from dif-  
980 ferent source models. In contrast, scaling the number of prompts involves a more complex pipeline  
981 that includes classification, filtering, and rewriting, which is significantly more resource-intensive.  
982

983 Despite this, FuseRL maintains strong alignment performance under constrained training budgets.  
984 As shown in Table 8, using only 15K prompts with 4 responses per prompt, our method matches the  
985 performance of baselines trained with 60K prompts and a single response. Moreover, while these  
986 baselines exhibit signs of performance saturation, FuseRL continues to benefit from larger datasets.  
987 When scaled to 60K prompts with 4 responses, FuseRL yields further improvements, highlighting  
988 its superior scaling potential. All experiments were conducted on a cluster of  $8 \times 80\text{GB}$  A800 GPUs.  
989

990 Table 8: FuseRL achieves competitive or superior performance with fewer prompts and more re-  
991 sponses, demonstrating better scalability compared to baseline methods.  
992

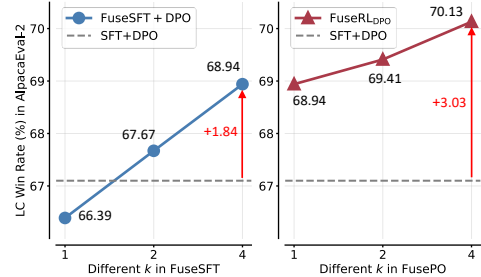
993 <b>Method</b>	<b>Prompts</b>	<b>Responses</b>	<b>Runtime (hrs)</b>	<b>AlpacaEval-2</b>	
				<b>LC (%)</b>	<b>WR (%)</b>
994 $\text{FuseRL}_{\text{DPO}}$	60K	4	11.5	<b>70.1</b>	70.9
	30K	4	6.2	69.0	72.5
	15K	4	3.8	64.2	69.2
995 $\text{SFT+DPO}$	60K	1	3.6	67.1	69.2
	60K	1	4.8	67.7	<b>74.2</b>

## 1001 H IMPACT OF DIFFERENT $k$ ON FUSERL 1002

1003 In this section, we examine the impact of varying  
1004 the number of responses and preference pairs, de-  
1005 noted as  $k$  (where  $1 \leq k \leq K$ ), on the final align-  
1006 ment performance of the target model in both stages  
1007 of FuseSFT and FusePO. Specifically,  $k$  in the Fus-  
1008 eSFT stage refers to the top- $k$  responses from all  
1009 source models used in Eq. (10), ranked by reward  
1010 scores, while in the FusePO phase, it represents pre-  
1011 ference pairs derived from the top- $k$  highest-scoring  
1012 source models used in Eq. (11). These variations in  
1013 the selection of responses and preference pairs are  
1014 evaluated to understand their influence on the align-  
1015 ment performance of the target model. As shown  
1016 in Figure 6, increasing  $k$  in both the FuseSFT and  
1017 FusePO stages leads to consistent performance im-  
1018 provement in the target model’s LC win rate. This  
1019 indicates that our method effectively leverages re-  
1020 sponses (even suboptimal responses and preference  
1021 pairs) from multiple source models for optimization.  
1022

## 1023 I TEMPERATURE COEFFICIENTS IN FUSERL

1024 The temperature coefficient play a crucial role in weighting the contributions of responses or  
1025 preference pairs from different source models, calculated using a softmax-based reward mecha-  
1026 nism as defined in Eq. (8). In this section, we examine the influence of different temperature



1027 Figure 6: The impact of varying the number  
1028 of responses or preference pairs of FuseSFT  
1029 and FusePO on the LC win rate. **Left:** Re-  
1030 sults for FuseSFT + DPO, where  $k$  denotes using  
1031 the top- $k$  responses from source models  
1032 during the FuseSFT stage. **Right:** Re-  
1033 sults for  $\text{FuseRL}_{\text{DPO}}$ , denoting using pre-  
1034 ference pairs derived from the top- $k$  highest-  
1035 rewarding source models for the FusePO.

coefficients on the performance of the FuseRL framework, which consists of two stages: FuseSFT and FusePO, with SFT+DPO serving as the baseline. The effect of temperature coefficients in the FuseSFT stage is demonstrated through the results of FuseSFT followed by off-policy DPO training. For the FusePO stage, we use the optimal settings identified for FuseSFT and analyze the influence of adjusting the temperature parameter on FusePO performance.

In Figure 7, we observe consistent performance improvements of FuseSFT and FusePO compared to the SFT+DPO baseline across a wide range of temperature settings. This clearly demonstrates the effectiveness of the reward-based weighting mechanism in integrating diverse information from heterogeneous source models, enabling the target model to achieve superior performance.

## J RESPONSES SELECTION STRATEGIES FOR FUSESFT

In this section, we analyze the impact of various response selection strategies on the performance of FuseSFT, focusing on how different methods influence the model’s alignment performance. To illustrate these effects, we present the results of FuseSFT trained with different strategies, along with the outcomes of subsequent DPO training. The first strategy, which serves as the default configuration, the top- $k$  responses from all available responses generated by the source models. In this case,  $k = 4$ , meaning the top four responses across all source models are chosen. The second strategy selects the top response from each source model, resulting in a total of four responses (one per source model). The results in Table 9 demonstrate a clear hierarchy: the top- $k$  selection strategy outperforms the top-1 selection per source model, regardless of the training stage. These findings highlight the critical importance of prioritizing high-quality responses during the alignment process. The top- $k$  selection strategy not only leverages the advantage of weighted responses from multiple source models but also consistently delivers the best results by utilizing the most informative and relevant responses.

## K SUPPLEMENTARY ANALYSIS OF FUSERL: REDUCING BIAS AND VARIANCE

In Section 4.5, we analyze the impact of FuseRL on reducing bias and variance by conducting analytical experiments. These experiments compare the responses generated by different approaches with the simulated ideal responses (by GPT4-Top1) on AlpacaEval-2. Below, we first detail the evaluation metrics, including absolute error, absolute bias, and variance:

- **Absolute Error:** The absolute difference between the preference scores of the response generated by the model under study and the response by GPT4-Top1.
- **Absolute Bias:** The mean of the absolute errors across all data points.
- **Variance:** The mean squared deviation of the absolute errors, indicating the consistency of the model’s predictions.

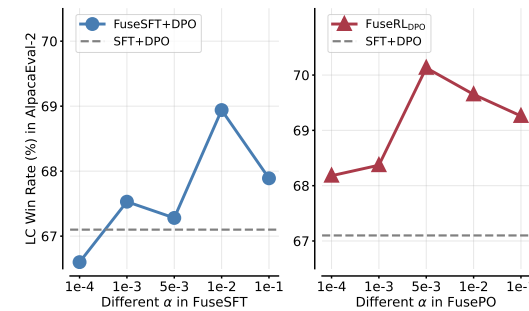


Figure 7: The influence of varying temperature coefficients  $\alpha$  on the performance of FuseRL, including FuseSFT and FusePO stages, on AlpacaEval-2.

Table 9: Comparison of different response selection strategies for FuseSFT on AlpacaEval-2.

Method	Settings	AlpacaEval-2	
		LC (%)	WR (%)
FuseSFT	Top- $k$ from all source models	<b>38.8</b>	<b>33.7</b>
	Top-1 from each source models	36.3	31.6
FuseSFT+DPO	Top- $k$ from all source models	<b>68.9</b>	<b>73.0</b>
	Top-1 from each source models	66.5	71.2
FuseRL-DPO	Top- $k$ from all source models	<b>70.1</b>	<b>70.9</b>
	Top-1 from each source models	68.7	70.2

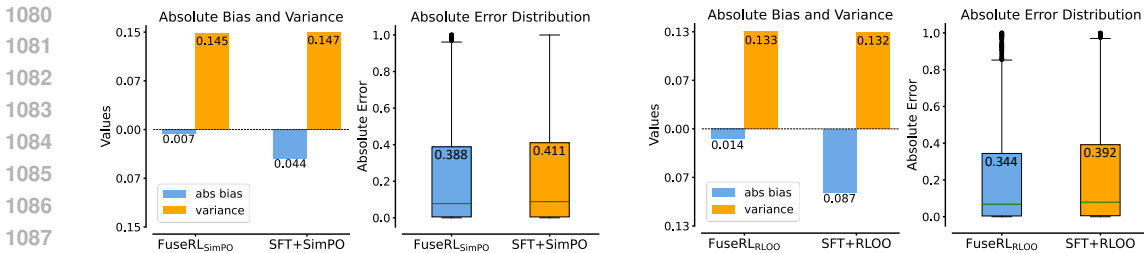


Figure 8: Comparison of absolute bias, variance, and absolute error distribution between FuseRL and baseline methods. **Left:** FuseRL<sub>SimPO</sub> vs. SFT+SimPO. **Right:** FuseRL<sub>RLOO</sub> vs. SFT+RLOO.

Furthermore, we present supplementary experimental results to further support our findings. In Figure 8 (Left), we compare FuseRL<sub>SimPO</sub> with the baseline, while in Figure 8 (Right), we compare FuseRL<sub>RLOO</sub> with SFT+RLOO.

These supplementary results demonstrate that FuseRL achieves measurable reductions in absolute bias compared to relying solely on the best individual source model for each prompt, highlighting its effectiveness in minimizing deviations between the generated and (simulated) ideal responses. Moreover, FuseRL (except for RLOO) demonstrates lower variance, indicating enhanced consistency and robustness in generating responses aligned with human preferences. However, while RLOO under the FuseRL framework achieves a substantial reduction in bias, its variance shows a slight increase. This can be attributed to two factors. First, due to computational resource limitations, RLOO uses only two responses per prompt, which restricts its overall performance and affects the variance scores. Second, there is an inherent trade-off between bias and variance—RLOO’s optimization strategy prioritizes minimizing bias, which increases sensitivity to input variations and leads to a slight rise in variance. Moreover, the absolute error distributions under FuseRL are consistently lower than those of the baseline methods, further emphasizing its ability to deliver stable and consistent performance across diverse inputs.